Transformations and Agostic Interactions of Hydrocarbyl Ligands Bonded to the Sulfur-Rich Dimolybdenum Site $\{Mo_2Cp_2(\mu\text{-}SMe)_3\}$: Chemical and Electrochemical Formation of μ-Alkyl and μ-Vinyl Compounds from a μ-Alkylidene Derivative

Nolwenn Cabon, Alan Le Goff, Christine Le Roy, François Y. Pétillon,* Philippe Schollhammer,* and Jean Talarmin*

UMR CNRS 6521, Chimie, Electrochimie Moléculaires et Chimie Analytique, UFR Sciences et Techniques, Université de Bretagne Occidentale, CS 93837, 29238 Brest-Cedex 3, France

John E. McGrady*

Department of Chemistry, University of York, Heslington, York Y010 5DD, U.K.

Kenneth W. Muir*

Chemistry Department, University of Glasgow, Glasgow G12 8QQ, U.K.

Received September 2, 2005

A series of chemical and electrochemical transformations of systems in which a $\{Mo_2Cp_2(\mu\text{-}SMe)_3\}$ core is bridged by a μ-C_2H_nR ligand ($n = 0-4$) are described in this paper. The reaction of the alkylidene complex $[Mo_2Cp_2(\mu\text{-}SMe)_3(\mu\text{-}\eta^1{:}\eta^2\text{-}CHCH_2Tol)](BF_4)$ (**1**) with $LiBu^n$ at 0 °C produces the μ-σ,π-vinyl complex $[Mo_2Cp_2(\mu\text{-}SMe)_3((\mu\text{-}\eta^1{:}\eta^2\text{-}CH{=}CHTol]$ (**2**) in good yield. The molecular structure of **2** has been confirmed by X-ray analysis. Upon treatment with $NaBH_4$ **1** is readily converted into the semibridging alkyl species $[Mo_2Cp_2(\mu\text{-}SMe)_3(\mu\text{-}CH_2CH_2Tol)]$ (**3**), which is also formed by electrochemical reduction of **1** in acidic medium. NMR and X-ray diffraction studies of **3** are consistent with, but do not definitively establish, the presence of a η^1 α-agostic interaction. Density functional theory has been used to confirm the presence of agostic interactions in both **1** and **3** and also to explore the exchange pathways for these hydrocarbyl dimolybdenum systems. Electrochemical transformation of the μ-alkylidene complex **1** gives **3** as the major product when acid is present and a mixture of **2** and **3** when acid is absent, production of **2** being favored by low initial concentrations of **1**. Theoretical, spectroscopic, and diffraction data are used to explain the formation and structures of closely related $[Mo_2Cp_2(\mu\text{-}SMe)_3(\mu\text{-}C_2H_nR]^{z+}$ complexes ($n = 0-4$ and $z = 0, 1$), including **1**−**3**.

Introduction

The search for new tools to activate molecules and for models which mimic the behavior of less accessible biological or industrial catalysts inspires current interest in the chemistry of polymetallic compounds.[1] For example, the bis(cyclopentadienyl) bimetallic fragments $\{M_2Cp'_2\}$ ($Cp' = \eta^5\text{-}C_5R_5$) exhibit significant metal−metal interactions and have a rich and original chemistry which merits further exploration.[2] As an illustration of this approach, we reported a sequence of transformations of unsaturated dinitrogenous substrates (RN=N, RN=NH) at a sulfur-rich dimolybde-

* To whom correspondence should be addressed. E-mail: françois.petillon@univ-brest.fr (F.Y.P.); schollha@univ-brest.fr (P.S.); jean.talarmin@univ-brest.fr (J.T.); jem15@york.ac.uk (J.E.M.); ken@chem.gla.ac.uk (K.W.M.).

(1) (a) *Catalysis by Di- and Polynuclear Metal Cluster Complexes*; Adams, R. D., Cotton, F. A., Eds.; Wiley-VCH: New York, 1998. (b) Braunstein, P.; Rose, J. In *Chemical Bonds-Better Ways to Make Them and Break Them*; Bernal, I., Ed.; Elsevier: Amsterdam, 1989; p 5. (c) Hidai, M.; Mizobe, Y. In *Transition Metal Sulfur Chemistry-Biological and Industrial Significance*; Stiefel, E. I., Matsumoto, K., Eds.; ACS Symposium Series 653; American Chemical Society: Washington, DC, 1996; p 310. (d) Hidai, M.; Mizobe, Y.; Matsuzaka , H. *J. Organomet. Chem.* **1994**, *473*, 1 and references therein.

(2) For recent examples and reviews: (a) Alvarez, C. M.; Alvarez, M. A.; Garcia, M. E.; Ramos, A.; Ruiz, M. A.; Lanfranchi, M.; Tiripicchio, A. *Organometallics* **2005**, *24*, 7. (b) Alvarez, C. M.; Garcia, M. E.; Rueda, M. T.; Ruiz, M. A.; Saez, D.; Connelly, N. G. *Organometallics* **2005**, *24*, 650. (c) Alvarez, M. A.; Anaya, Y.; Garcia, M. E.; Ruiz, M. A. *Organometallics* **2004**, *23*, 3950. (d) Alonso, M.; Garcia, M. E.; Ruiz, M. A.; Hamidov, H.; Jeffery, J. C. *J. Am. Chem. Soc.* **2004**, *126*, 13610. (e) Cabon, N.; Pétillon, F. Y.; Schollhammer, P.; Talarmin, J.; Muir, K. W. *Dalton Trans.* **2004**, 2708. (f) Nishibayashi, Y.; Imajima, H.; Onodera, G.; Hidai, M.; Uemura, S. *Organometallics* **2004**, *23*, 26. (g) Nishioka, T.; Kitayama, H.; Breedlove, B. K.; Shiomi, K.; Kinoshita, I.; Isobe, K. *Inorg. Chem.* **2004**, *43*, 5688. (h) Adams, H.; Morris, M. J.; Morris, S. A.; Motley, J. C. *J. Organomet. Chem.* **2004**, *689*, 522. (i) Cremer, C.; Burger, P. *Chem. Eur. J.* **2003**, *9*, 3583. (j) Nishibayashi, Y.; Yoshikawa, M.; Inada, Y.; Hidai, M.; Uemura, S. *J. Am. Chem. Soc.* **2002**, *124*, 11846. (k) Bridgeman, A. J.; Mays, M. J.; Woods, A. D. *Organometallics* **2001**, *20*, 2076. (l) Hobert, S. E.; Bruce, C.; Noll, B. C.; Rakowski DuBois, M. *Organometallics* **2001**, *20*, 1370. (m) Adams, H.; Allott, C.; Bancroft, M. N.; Morris, M. J. *Dalton Trans.* **2000**, 4145. (n) Pétillon, F. Y.; Schollhammer, P.; Talarmin, J.; Muir, K. W. *Coord. Chem. Rev.* **1998**, *178*−*180*, 203. (o) Rakowski DuBois, M. *Polyhedron* **1997**, *16*, 3089. (p) Rakowski DuBois, M. *J. Cluster Sci.* **1996**, *7*, 293. (q) Hidai, M.; Mizobe, Y.; Matsuzaka, H. *J. Organomet. Chem.* **1994**, *473*, 1. (r) Winter, M. J. *Adv. Organomet. Chem.* **1989**, *29*, 101. (s) Curtis, M. D. *Polyhedron* **1987**, *6*, 759.

10.1021/om050761g CCC: $30.25
Publication on Web 11/04/2005

Scheme 1. Successive Transformations of Hydrocarbyl Bridges at the $\{Mo_2Cp_2(\mu\text{-}SMe)_3\}$ Group

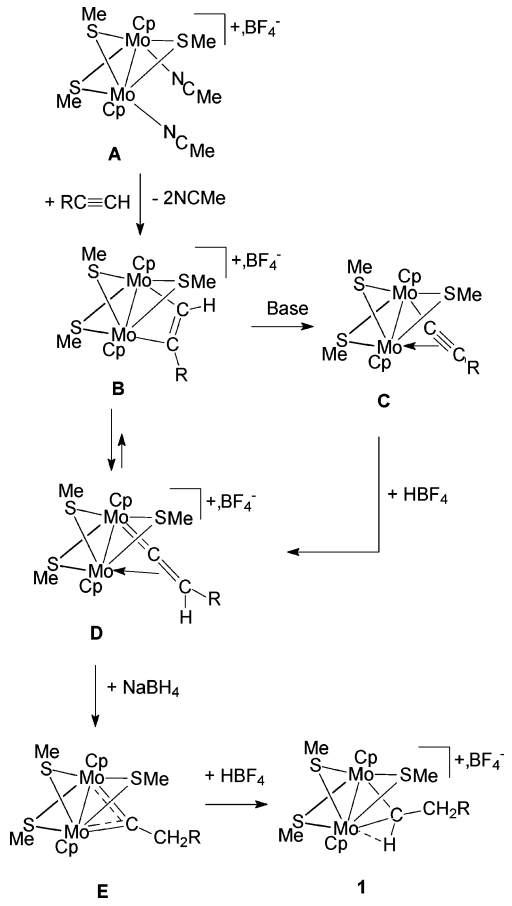

num site $\{Mo_2Cp_2(\mu\text{-}SMe)_3\}$[3] which suggests a completely novel pathway for the reduction of N_2 at a dinuclear site of FeMoco.[3a,b,4] Very recently we have used density functional theory to explore the electronic pathways involved in these reduction processes.[5]

We have also described the activation of other small, unsaturated molecules, such as terminal alkynes (HC≡CR) (Scheme 1),[6] isocyanides (RN≡C),[7] and nitriles (RC≡N), by the $\{Mo^{III}_2Cp_2\}$ system.[8] The conversion of the alkyne adduct $[Mo_2Cp_2(\mu\text{-}SMe)_3(HC{\equiv}CR)](BF_4)$ (**B**; Cp = η^5-C_5H_5) into the readily accessible vinylidene derivative $[Mo_2Cp_2(\mu\text{-}SMe)_3(\mu\text{-}\eta^1{:}\eta^2\text{-}C{=}CHR)](BF_4)$ (**D**) (Scheme 1) was the starting point for new studies[6] focused on the transformations of hydrocarbyl groups at this sulfur-rich site. There have been few systematic studies of complexes featuring $\{M_2(\mu\text{-}\eta^1{:}\eta^2\text{-}C{=}CHR)\}$ groups,[9] and it remains unclear whether the $\eta^1{:}\eta^2$ coordination mode induces novel reactivity in the vinylidene moiety or is, instead, a dead end in its transformation pathway. In addition to the fundamental interest in this chemistry, the transformations of RC≡CH may also shed some light on the biologically and industrially critical activation of the isoelectronic N≡N bond. The investigation of reactions of **D** with various nucleophilic reagents has been the focus of our studies so far.[6a,c] The formal addition of hydride to the outer carbon atom of the vinylidene bridge in **D** resulted in the formation of μ-alkylidyne derivatives $[Mo_2Cp_2(\mu\text{-}SMe)_3(\mu\text{-}CCH_2R)]$ (**E**). The electrochemical conversion of **D** into **E** will be reported in a separate paper.[10] **E** was readily protonated, forming the μ-alkylidene species $[Mo_2(\eta^5\text{-}C_5H_5)_2(\mu\text{-}SMe)_3(\mu\text{-}\eta^1{:}\eta^2\text{-}CHCH_2R)](BF_4)$ (**1**), which, according to NMR evidence, exhibits α-agostic interactions.[6a]

The reactivity of the μ-alkylidene derivative $[Mo_2Cp_2(\mu\text{-}SMe)_3(\mu\text{-}\eta^1{:}\eta^2\text{-}CHCH_2R)](BF_4)$ (**1**; R = Ph, tolyl) forms the basis of the current paper. We describe the deprotonation of **1** by $LiBu^n$, leading to the μ-σ,π-vinyl complex $[Mo_2Cp_2(\mu\text{-}SMe)_3((\mu\text{-}\eta^1{:}\eta^2\text{-}CH{=}CHR]$ (**2**), as well as its chemical reduction with sodium borohydride (R = Tol) and its electrochemical reduction in acidic solution (R = Ph), leading to the semibridging alkyl derivative $[Mo_2Cp_2(\mu\text{-}SMe)_3(\mu\text{-}CH_2CH_2R)]$ (**3**). NMR evidence suggests that **3**, like **1**, is stabilized by α-agostic interactions. The remarkable diversity of hydrocarbyl coordination environments illustrated in this and previous papers, along with their apparently facile interconversion, has also prompted us to use theoretical methods to investigate their structure and dynamics.

Results and Discussion

1. Computed Structure of the Alkylidene Cation $[Mo_2Cp_2(\mu\text{-}SH)_3(\mu\text{-}CHCH_2Ph)]^+$. As noted above, the alkylidene species $[Mo_2Cp_2(\mu\text{-}SMe)_3(\mu\text{-}CHCH_2Tol)](BF_4)$ (**1**) forms the foundation of the current studies. Although we have characterized **1** thoroughly by NMR spectroscopy, we have been unable to obtain crystals suitable for X-ray analysis.

A logical starting point for the computational component of the study is therefore the structure of the model cation $[Mo_2Cp_2(\mu\text{-}SH)_3(\mu\text{-}CHCH_2Ph)]^+$ (**1′**), where the methyl substituents on the phenyl and sulfido ligands have been removed for computational expedience. Our previous experience in closely related systems suggests that this simplification should not have a dramatic influence on the structure.[5] In all cases, the prime (′) signifies that the methyl groups have been removed. The optimized structure of **1′**, shown in Figure 1, confirms the highly asymmetric nature of the alkylidene bridge, with Mo(1)−C_α and Mo(2)−C_α bond lengths of 1.95 and 2.39 Å, respectively. The very short bond length is indicative of substantial Mo=C multiple bonding, simi-

(3) (a) Le Grand, N.; Muir, K. W.; Pétillon, F. Y.; Pickett, C. J.; Schollhammer, P.; Talarmin, J. *Chem. Eur. J.* **2002**, *8*, 3115. (b) Pétillon, F. Y.; Schollhammer, P.; Talarmin, J. *Inorg. Chem.* **1999**, *38*, 1954. (c) Schollhammer, P.; Didier, B.; Le Grand, N.; Pétillon, F. Y.; Talarmin, J.; Muir, K. W.; Teat, S. J. *Eur. J. Inorg. Chem.* **2002**, 658. (d) Schollhammer, P.; Guénin, E.; Pétillon, F. Y.; Talarmin, J.; Muir, K. W. *Organometallics* **1998**, *17*, 1922.

(4) (a) Durrant, M. C. *Inorg. Chem. Commun.* **2001**, *4*, 60. (b) Barrière, F. *Coord. Chem. Rev.* **2003**, *236*, 71.

(5) McGrady, J. E.; Padden Metzker, J. K. *Chem. Eur. J.* **2004**, *10*, 6447.

(6) (a) Cabon, N.; Schollhammer, P.; Pétillon, F. Y.; Talarmin, J.; Muir, K. W. *Organometallics* **2002**, *21*, 448. (b) Schollhammer, P.; Cabon, N.; Capon, J. F.; Pétillon, F. Y.; Talarmin, J.; Muir, K. W. *Organometallics* **2001**, *20*, 1230. (c) Schollhammer, P.; Cabon, N.; Kervella, A.-C.; Pétillon, F. Y.; Rumin, R.; Talarmin, J.; Muir, K. W. *Inorg. Chim. Acta* **2003**, *350*, 495.

(7) Cabon, N.; Paugam, E.; Pétillon, F. Y.; Schollhammer, P.; Talarmin, J.; Muir, K. W. *Organometallics* **2003**, *22*, 4178.

(8) (a) Schollhammer, P.; Le Hénanf, M.; Le Roy-Le Floch, C.; Pétillon, F. Y.; Talarmin, J.; Muir, K. W. *Dalton Trans.* **2001**, 1573. (b) Schollhammer, P.; Pichon, M.; Muir, K. W.; Pétillon, F. Y.; Pichon, R.; Talarmin, J. *Eur. J. Inorg. Chem.* **1999**, 221.

(9) (a) Bruce, M. I. *Chem. Rev.* **1991**, *91*, 197. (b) El Amouri, H.; Gruselle, M. *Chem. Rev.* **1996**, *96*, 1077.

(10) Le Goff, A.; Le Roy, C.; Pétillon, F. Y.; Schollhammer, P.; Talarmin, J., Manuscript in preparation.

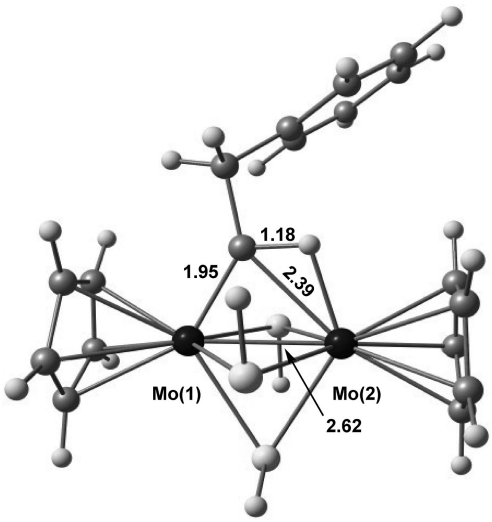

Figure 1. Optimized structure of $[Mo_2Cp_2(\mu\text{-}SH)_3(\mu\text{-}CHCH_2\text{-}Ph)]^+$ (**1′**).

lar to that observed in the related alkylidyne ($[Mo_2Cp_2(\mu\text{-}SMe)_3(\mu\text{-}CCH_2n\text{-}Pr)]$) and vinylidene ($[Mo_2Cp_2(\mu\text{-}SMe)_3(\mu\text{-}CCHTol)]^+$) species.[6a,b] The elongated $C_\alpha-H$ bond (1.18 Å) and the acute $Mo(2)-C_\alpha-H$ angle (50.1°) are indicative of a significant agostic interaction with the electron-deficient molybdenum center. However, it should be noted that the $Mo(1)-C_\alpha-H$ angle (122°) is nearly identical with the ideal sp^2 value of 120°, suggesting that the acute $Mo(2)-C_\alpha-H$ angle is a consequence of the optimization of the $Mo(1)-C_\alpha$ bonding rather than an indication of any intrinsically strong interaction between the C−H group and the metal center. Similar features were noted in one of the earliest studies of agostic bonding, where Eisenstein and coworkers showed that the α-agostic distortion in $H_5TaCH_3^-$ is driven by the optimization of M−C, rather than C−H···M bonding.[11] As noted in ref 6a, only a single Cp resonance was observed down to 213 K for **1**, suggesting that the complex is highly fluxional. We will return to this issue following a discussion of the formation of **2** and **3** from **1**.

2. Reaction of $[Mo_2Cp_2(\mu\text{-}SMe)_3(\mu\text{-}CHCH_2Tol)](BF_4)$ (1) with $LiBu^n$. Spectroscopic Characterization and Molecular Structure of $[Mo_2Cp_2(\mu\text{-}SMe)_3(\mu\text{-}\eta^1{:}\eta^2\text{-}CH{=}CHTol)]$ (2). The reaction of the μ-alkylidene compound $[Mo_2Cp_2(\mu\text{-}SMe)_3(\mu\text{-}CHCH_2Tol)](BF_4)$, (**1**), with a slight excess of $LiBu^n$ (1.5 equiv) in tetrahydrofuran at 273 K, resulted in the formation of the μ-vinyl derivative $[Mo_2Cp_2(\mu\text{-}SMe)_3((\mu\text{-}\eta^1{:}\eta^2\text{-}CH{=}CHTol)]$ (**2**), which was isolated in good yield (91%) (reaction 1).

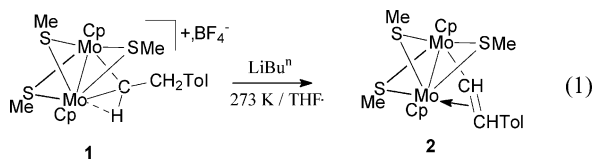

1 2 (1)

2 was characterized by elemental analysis and ^1H NMR spectroscopy, which exhibits the sets of resonances expected for the $\{Mo_2Cp_2(\mu\text{-}SMe)_3\}$core and the tolyl group. Only one signal was observed for cyclopentadienyl groups, in CD_2Cl_2 down to 220 K, indicating that the dynamic process remains rapid at low temperature and, hence, cannot be studied on the NMR time scale. The vinyl bridge ($\mu\text{-}\eta^1{:}\eta^2$-CH=CHTol) was characterized by the observation of two doublets at 7.18 and 6.73 ppm with a coupling constant $^3J_{HH}$ of 15 Hz, indicating a trans disposition of the vinyl hydrogen atoms. Two-dimensional heteronuclear inverse-correlation $^1H-^{13}C$ experiments (HMQC, HMBC) allowed further characterization of **2**. The ^{13}C chemical shifts for σ-bonded (C_α) and non-σ-bonded (C_β) carbon atoms of the μ-vinyl group appear at 153.8 and 104.8 ppm, respectively, suggesting there is little contribution from a carbene-like canonical form to **2**.[12] The structure of **2** (Figure 2 and Table 1) was confirmed by X-ray analysis of a single crystal obtained from a diethyl ether solution at room temperature. This establishes that **2** contains a unsymmetrical σ,π-CH=CHTol group which bridges the Mo−Mo bond of the $\{Mo^{III}_2Cp_2(\mu\text{-}SMe)_3\}$ core. The length of the Mo−Mo bond (2.601(1) Å) is unexceptional, as are those of the μ-Mo−S bonds, which fall in the range 2.445(3)−2.482(2) Å, apart from the somewhat longer Mo(1)−S(2) distance of 2.533(2) Å.[2n] The three-electron-donor vinyl ligand bonds terminally to Mo(2) (Mo(2)−C(4) = 2.204(9) Å) and via a weak unsymmetrical π-interaction to Mo(1) (Mo(1)−C(4) = 2.320(9) and Mo(1)−C(5) = 2.528(9) Å). The C(4)−C(5) vinyl bond length (1.371(12) Å) agrees with values in related vinylidene species (1.356-

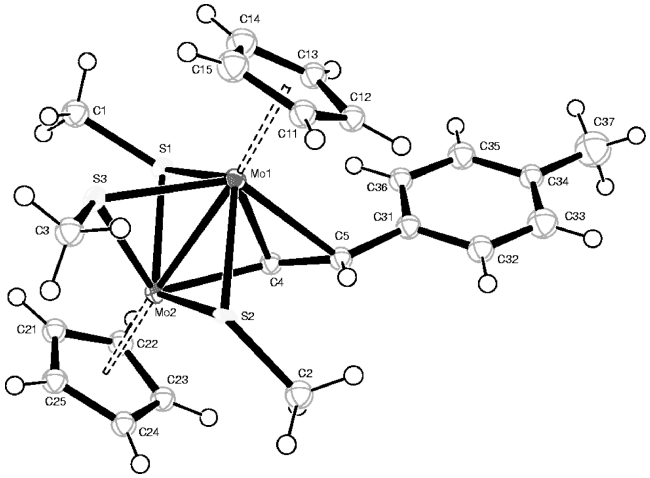

Figure 2. ORTEP drawing of complex **2** showing 20% probability ellipsoids**.** The hydrogen atom on C(4) was not located.

Table 1. Selected Bond Lengths (Å) and Angles (deg) for $[Mo_2Cp_2(\mu\text{-}SMe)_3(\mu\text{-}\eta^1{:}\eta^2\text{-}CH{=}CHTol)]$ (2)

Mo(1)−S(1)	2.482(2)	Mo(2)−S(1)	2.455(2)
Mo(1)−S(2)	2.533(2)	Mo(2)−S(2)	2.445(3)
Mo(1)−S(3)	2.448(2)	Mo(2)−S(3)	2.457(2)
Mo(1)−C(4)	2.320(9)	Mo(2)−C(4)	2.204(9)
Mo(1)−C(5)	2.528(9)	C(4)−C(5)	1.371(12)
Mo(1)−Mo(2)	2.601(1)	C(5)−C(31)	1.510(9)
Mo(1)−C(4)−C(5)	82.1(5)	Mo(2)−C(4)−C(5)	133.6(7)
		C(4)−C(5)−C(31)	123.9(7)
Mo(1)−C(4)−C(5)−C(31)		−117.5(7)	
C(4)−C(5)−C(31)−C(32)		−156.4(7)	
Mo(2)−C(4)−C(5)−C(31)		−170.2(6)	

(11) Demolliens, A.; Jean, Y.; Eisenstein, O. *Organometallics* **1986**, *5*, 1457.

(12) Schollhammer, P.; Pétillon, F. Y.; Poder-Guillou, S.; Talarmin, J.; Muir, K. W.; Yufit, D. S. *J. Organomet. Chem.* **1995**, *513*, 181 and references therein.

Table 2. Selected Bond Lengths (Å) and Angles (deg) for [$Mo_2Cp_2(\mu\text{-}SMe)_3(\mu\text{-}CH_2CH_2Tol)$] (3)

Mo(1)−S(1)	2.441(2)	Mo(2)−S(1)	2.438(2)
Mo(1)−S(2)	2.454(2)	Mo(2)−S(2)	2.449(2)
Mo(1)−S(3)	2.447(2)	Mo(2)−S(3)	2.467(3)
Mo(1)−C(4)	2.448(8)	Mo(2)−C(4)	2.285(7)
Mo(1)−Mo(2)	2.573(1)	C(4)−C(5)	1.509(11)
		C(5)−C(6)	1.495(12)
Mo(1)−C(4)−C(5)	127.0(5)	Mo(2)−C(4)−C(5)	122.8(5)
C(4)−C(5)−C(6)	111.9(7)	C(5)−C(6)−C(7)	121.8(8)
Mo(1)−C(4)−C(5)−C(6)		108.1(7)	
C(4)−C(5)−C(6)−C(7)		−97.7(10)	
Mo(2)−C(4)−C(5)−C(6)		−169.1(5)	

(6) Å) (Table 3) and in other μ-σ,π-vinyl complexes.[12] The Mo(2)−C(4)−C(5)−C(31) torsion angle of −170.2(6)° is consistent with the trans arrangement of protons attached to C(4) and C(5) deduced from NMR. Comparison of the structural features of the {$Mo_2(\mu\text{-}\eta^1\text{:}\eta^2\text{-}C_\alpha H{=}C_\beta HR)$} core of **2** with that of the vinylidene moiety {$Mo_2(\mu\text{-}\eta^1\text{:}\eta^2\text{-}C_\alpha{=}C_\beta HR)$} in [$Mo_2Cp_2(\mu\text{-}SMe)_3(\mu\text{-}\eta^1\text{:}\eta^2\text{-}C{=}CHPh)](BF_4)$ (**D**) (Table 3) reveals that the formal addition of H^- to C_α in **D** to give **2** increases the Mo(2)−C_α bond length from 1.894(5) Å in **D** to 2.204(9) Å in **2**. As expected, the Mo(2)−C_α−C_β angle of 164.6(4)° in **D** decreases to 133.6(7)° in **2**. However, the Mo−C_α and Mo−C_β lengths of 2.268(5) and 2.589(5) Å in **D** are broadly comparable with the corresponding values in **2**.

The optimized structure of the model μ-vinyl compound [$Mo_2Cp_2(\mu\text{-}SH)_3((\mu\text{-}\eta^1\text{:}\eta^2\text{-}CH{=}CHPh)$] (**2′**) is summarized in Figure 3, and all bond lengths are in good agreement with the X-ray structure. Significantly, the

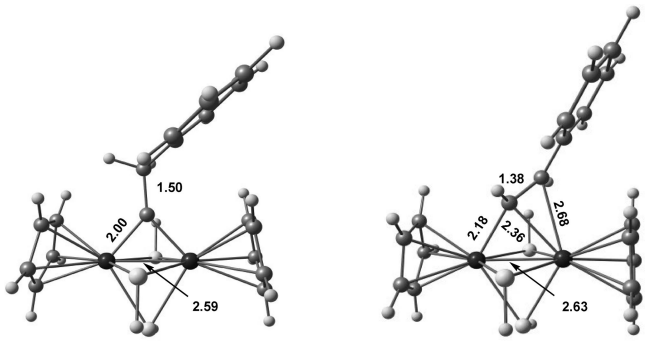

E' 2'

Figure 3. Optimized structures of [$Mo_2Cp_2(\mu\text{-}SH)_3(\mu\text{-}\eta^1\text{:}\eta^2\text{-}CH{=}CHPh)$] (**2′**) and [$Mo_2Cp_2(\mu\text{-}SH)_3(\mu\text{-}CCH_2Ph)$] (**E′**).

Mo−C bonds are much less asymmetric in **2′** than in **1′**, indicating much reduced Mo=C π bonding in the μ-vinyl species. Perhaps the most interesting aspect of the electronic structure of **2** is its comparison with the isomeric alkylidyne [$Mo_2Cp_2(\mu\text{-}SMe)_3((\mu\text{-}CCH_2Tol)$] (**E**), reported in ref 6a. **2** is formed by deprotonation of **1**, which is itself synthesized by the protonation of **E**. The optimized structure of the model alkylidyne [$Mo_2Cp_2(\mu\text{-}SH)_3(\mu\text{-}CCH_2Ph)$] (**E′**) is also shown in Figure 3, and the structure of the core is also in excellent agreement with the available X-ray data (for [$Mo_2Cp_2(\mu\text{-}SMe)_3(\mu\text{-}CCH_2Pr^n)$]).[6a] The μ-vinyl species **2′** is more stable than the μ-alkylidyne isomer, but only by 7 kJ mol^{-1}. However, if the phenyl group is replaced by hydrogen, the order of stability is reversed, with the μ-alkylidyne species being 28 kJ mol^{-1} lower than its μ-vinyl coun-

Table 3. Selected Distances (Å) and Angles (deg) in Hydrocarbyl Groups Bridging a [$Mo_2Cp_2(\mu\text{-}SMe)_3$] Core[a]

	Mo2C$_\alpha$	Mo1C$_\alpha$	Mo1C$_\beta$	C$_\alpha$C$_\beta$	Mo1Mo2	Mo2C$_\alpha$C$_\beta$
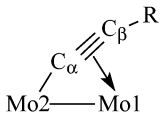 **C**	2.068(3)	2.360(3)	2.661(3)	1.238(4)	2.616(1)	160.9(3)
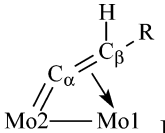 **D**	1.894(5)	2.268(5)	2.589(5)	1.356(6)	2.622(1)	164.6(4)
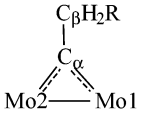 **E**	1.994(2)	1.996(2)		1.492(5)	2.585(1)	138.6(1) 140.5(1)
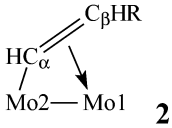 **2**	2.204(9)	2.320(9)	2.528(9)	1.371(12)	2.601(1)	133.6(7)
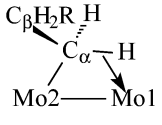 **3**	2.285(7)	2.448(8)	3.57(1)	1.509(11)	2.573(1)	122.8 (5) 127.0(5)

[a] Data are taken from the following: **C** and **D**, ref 6b; **E**, ref 6a; **2** and **3**, this work.

terpart, presumably due to the absence of conjugation of the C═C double bond. The computed energies therefore suggest that the balance between the μ-alkylidyne and μ-vinyl isomers is a delicate one and that subtle changes in composition are sufficient to tip the balance in favor of one or the other.

3. Reaction of $[Mo_2Cp_2(\mu\text{-}SMe)_3(\mu\text{-}CHCH_2Tol)](BF_4)$ (1) with $NaBH_4$. Spectroscopic Characterization and Molecular Structure of $[Mo_2Cp_2(\mu\text{-}SMe)_3(\mu\text{-}CH_2CH_2Tol)]$ (3). Compound **1** reacted with an excess of sodium borohydride in tetrahydrofuran at room temperature to afford a mixture of three products, $[Mo_2Cp_2(\mu\text{-}SMe)_3(\mu\text{-}CH{=}CHTol)]$ (**2**) and $[Mo_2Cp_2(\mu\text{-}SMe)_3(\mu\text{-}CCH_2Tol)]$ (**E**), both of which were characterized by comparison of their ^1H NMR spectra with those of authentic samples,[6] along with the novel species $[Mo_2Cp_2(\mu\text{-}SMe)_3(\mu\text{-}CH_2CH_2Tol)]$ (**3**) (reaction 2). The ratio

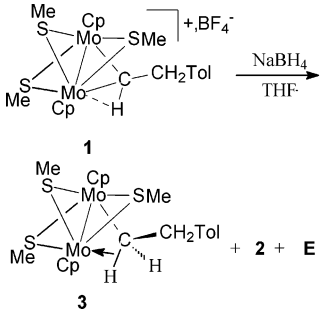

(2)

of the three species, **2**:**E**:**3**, is 33:10:57, confirming that the reduced species is the dominant product.

We assume that the formation of the side product **2** arose from β-deprotonation of **1**, as described previously, while **E** could form either by competitive α-deprotonation or by the reduction of $\mathbf{E}^+$, which is formed as a byproduct (in low yields) of the protonation of **E** in the preparation of **1**.[13] The transfer of a hydride to the bridging carbene of **1** gives rise to the novel derivative **3**. This complex was isolated as a green powder in only moderate yields (29%) following chromatographic workup, due to partial decomposition on the silica gel column. **3** was formulated as $[Mo_2Cp_2(\mu\text{-}SMe)_3(\mu\text{-}CH_2CH_2Tol)]$ on the basis of its spectroscopic and analytical data and solid-state structure. In addition to the expected signals for a $\{Mo_2Cp_2(\mu\text{-}SMe)_3\}$ core and the tolyl group, the ^1H NMR spectrum displayed two signals attributable to two methylene groups. One of these signals is observed at 2.42 ppm as a pseudo-triplet with a coupling constant (J_{HH}) of 6.6 Hz, while the second appears as a broad, unresolved resonance at −5.57 ppm. ^{13}C NMR and HMQC $^1H-^{13}C$ experiments suggested the presence of a semibridging alkyl ligand. The HMQC $^1H-^{13}C$ spectrum indicated that the two protons at −5.57 ppm were attached to a shielded carbon atom which resonates at 1.9 ppm. The value of the coupling constant $^1J_{CH}$ (112.2 Hz) of the α-methylenic group in the $\{Mo_2(\mu\text{-}C_\alpha H_2C_\beta H_2R)\}$ backbone, determined by recording the ^{13}C NMR spectrum of **3** without ^1H decoupling, is low compared with both the $^1J_{CH}$ value found for the β-methylenic group of the $\{Mo_2(\mu\text{-}C_\alpha H_2C_\beta H_2R)\}$ bridge (129.2 Hz) and with values generally observed for $C(sp^3)-H$ bonds.[14,15a] A single resonance was observed for the two cyclopentadienyl groups, suggesting either that the alkyl bridge is symmetrically bonded to the Mo_2 unit or that this group is fluxional in solution at room temperature. The available spectroscopic data are therefore consistent with the presence of an alkyl bridge and also suggest the presence of an α-agostic interaction but are insufficient to determine unambiguously the coordination mode of the $-CH_2CH_2Tol$ group. A few complexes in which an alkyl group (R = CH_3, generally) bridges middle or late transition metals have been reported and structurally characterized.[15] Of the various modes of coordination which have been proposed for the μ-alkyl ligand, only three could be consistent with the semibridging alkyl ligand in **3** (Chart 1): (a) symmetric pyramidal, (b) η^1 agostic, and (c) η^2 agostic. Note that only in (a) and (c) does the R−C bond lie in the $Mo_2(\mu\text{-}C)$ plane.

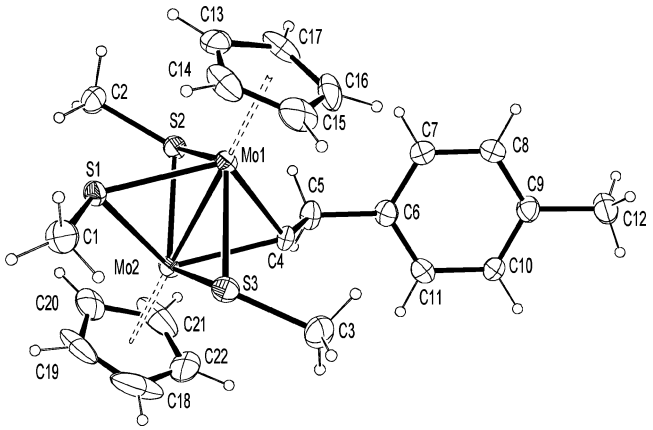

Figure 4. ORTEP drawing of complex **3** showing 20% probability ellipsoids. The hydrogen atoms on C(4) were not located.

Chart 1

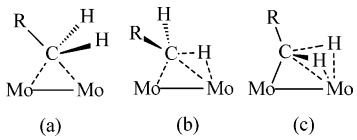

An X-ray analysis of a single crystal of **3** (Figure 4 and Table 3) obtained from a diethyl ether solution at room temperature confirmed that the bridging carbon is notably asymmetric (Mo(2)−C(4) = 2.285(7) Å and Mo(1)−C(4) = 2.448(8) Å), thereby excluding the symmetric pyramidal mode of coordination (a) and confirming the semibridging nature of the alkyl bridge. Other distances and angles (Table 2) are consistent with the proposed formulation $[Mo_2Cp_2(\mu\text{-}SMe)_3(\mu\text{-}CH_2CH_2Tol)]$. Although the analysis did not allow the positions of the two hydrogen atoms attached to C(4) to be determined experimentally, it does establish that the CH_2Tol group is oriented so that the C(4)−C(5) bond is nearly normal to the $Mo_2C(4)$ plane (Mo(2)−Mo(1)−C(4)−C(5) = 113.8(7)°), consistent only with (b) in Chart 1. This implies

(13) Le Goff, A.; Le Roy, C.; Pétillon, F. Y.; Schollhammer, P.; Talarmin, J. Manuscript in preparation.

(14) Martin, M. L.; Martin, C. J. In *Manuel de résonnance magnétique nucléaire*; Azoulay, Ed.; Paris, 1971.

(15) (a) Shin, J. H.; Parkin, G. *Chem. Commun.* **1998**, 1273. (b) Baik, M.-H.; Friesner, R. A.; Parkin, G. *Polyhedron* **2004**, 2879 and references therein. (c) Braunstein, P.; Boag, N. M. *Angew. Chem., Int. Ed.* **2001**, *40*, 2427 and references therein. (d) Bursten, B. E.; Cayton, R. H. *J. Am. Chem. Soc.* **1986**, *5*, 1051. (e) Garcia, M. A.; Melon, S.; Ramos, A.; Riera, V.; Ruiz, M. A.; Belleti, D.; Graiff, C.; Tiripicchio, A. *Organometallics* **2003**, *22*, 1983. (f) Dawkins, G. M.; Green, M.; Orpen, A. G.; Stone, F. G. A. *J. Chem. Soc., Chem. Commun.* **1982**, 41.

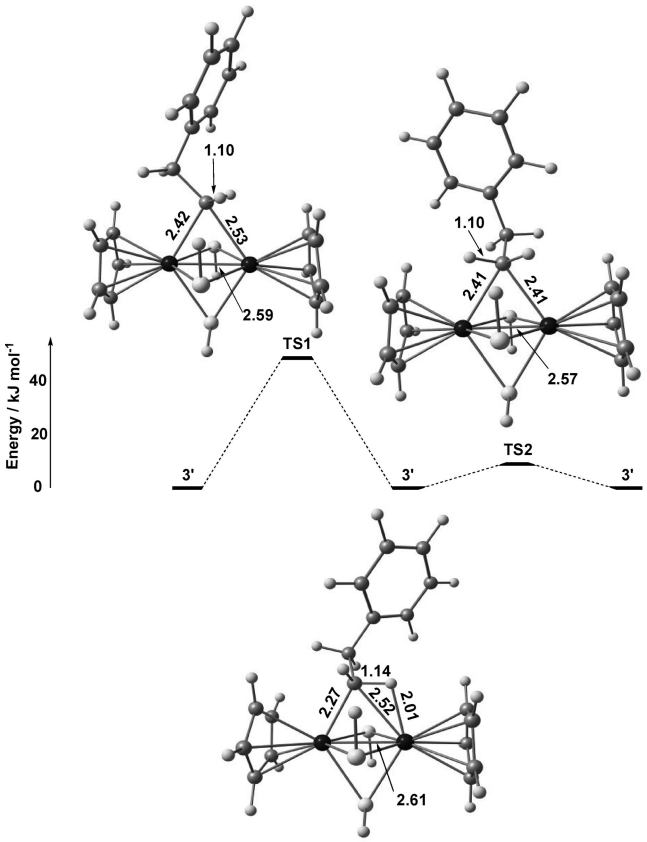

Figure 5. Potential energy surface for exchange of agostic and nonagostic C−H bonds in [$Mo_2Cp_2(\mu\text{-}SH)_3(\mu\text{-}CH_2CH_2Ph$)].

that only one C−H bond interacts with a Mo center. A survey of the potential energy surface of the model alkyl complex [$Mo_2Cp_2(\mu\text{-}SH)_3(\mu\text{-}CH_2CH_2Ph$)] (**3′**) confirms that, of the three possibilities shown in Chart 1, only (b) corresponds to a minimum. The optimized structure (Figure 5) is fully consistent with the X-ray data and, most significantly, firmly locates one C−H bond parallel to the Mo−Mo axis (C−H = 1.14 Å vs 1.10 Å for its nonagostic counterpart). A second α-C−H agostic minimum, related to **3′** by a clockwise 120° rotation of the bridging $-CH_2CH_2Ph$ group shown in Figure 5, has also been located only 2 kJ mol^{-1} higher in energy. The small energy difference between the two isomers arises from greater steric repulsions between the phenyl and S−H groups in the less stable isomer. In both isomers, the Mo(1)−C_α−H angle is 116°, only slightly increased from the ideal sp^3 angle of 109.5°, suggesting that the tilting of the alkyl group is a consequence of the optimization of the Mo(1)−C_α bonding rather than any intrinsically strong C−H···Mo interaction.

In contrast, structure (c) in Chart 1, formed by an anticlockwise 60° rotation of the bridging $-CH_2CH_2Ph$ group, corresponds to a transition state (**TS1**) on the potential energy surface, linking the two α-C−H agostic minima described above. However, this transition state cannot account for the observed fluxionality, because it does not interconvert the two metal centers (and hence the Cp groups). Moreover, **TS1** lies 46 kJ mol^{-1} above the minimum, a significant barrier that is inconsistent with the observation of equivalent Cp groups down to 213 K. We have, however, also located a second transition state, **TS2**, corresponding to a clockwise 60° rotation, which makes both the C−H bonds and the Cp groups equivalent. **TS2** lies only 13 kJ mol^{-1} above the ground state, and so is fully consistent with the persistence of fluxionality even at low temperatures.

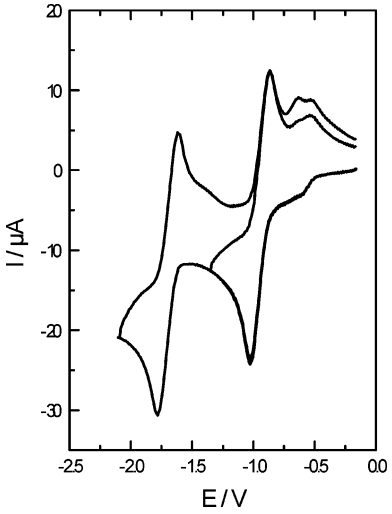

Figure 6. Cyclic voltammetry of [$Mo_2Cp_2(\mu\text{-}SMe)_3(\mu\text{-}\eta^1\text{:}\eta^2\text{-}CHCH_2Ph)$]$^+$ (**1**; ca. 1 mM) in CH_2Cl_2−[NBu_4][PF_6] (vitreous carbon electrode, v = 0.2 V s^{-1}).

4. Reductive Electrochemistry of [$Mo_2Cp_2(\mu\text{-}SMe)_3(\mu\text{-}CHCH_2R)$][$BF_4$] (1). We have previously reported the electrochemistry of various nitrogenous ligands bound to the {$Mo_2Cp_2(\mu\text{-}SMe)_3$} core and demonstrated that the N=N bond of a $\mu\text{-}\eta^1\text{:}\eta^1$-phenyldiazene bridge could be cleaved by controlled-potential reduction of the phenyldiazene complex in acidic solution.[3]

The synthesis of a wide variety of compounds bearing hydrocarbyl ligands resulting from the progressive reduction of a C≡C triple bond (μ-acetylide or μ-alkyne complexes)[6] gives us the opportunity to investigate their interconversion by electrochemical routes. This section focuses on one particular step of the overall C≡C reduction process: the electrochemical reduction of a μ-alkylidene derivative **1** to μ-vinyl (**2**) and μ-alkyl (**3**) complexes. The electrochemistry of μ-acetylide, μ-vinylidene, and μ-alkylidyne complexes will be reported separately.[10,13]

Although it is clear that the electrochemical conversion of a μ-alkylidene bridge to an alkyl ligand will take place more favorably in the presence of protons, we will first present the electrochemistry of the μ-alkylidene complex **1** in the absence of acid.

The μ-alkylidene complex **1** with R = Ph or R = Tol presents similar cyclic voltammetry in CH_2Cl_2−[NBu_4]-[PF_6]. The detailed electrochemical study was carried out with the phenyl-substituted derivative. This complex undergoes two one-electron reduction steps, at $E_{1/2}^{red1} = -0.95$ V and $E_{1/2}^{red2} = -1.72$ V (Figure 6, Scheme 2), as well as two irreversible oxidations at $E_p^{ox1} = 0.56$ V and $E_p^{ox2} = 0.81$ V.[16] Both reduction steps are essentially reversible electrochemically with ΔE_p = 80 mV at v = 0.2 V s^{-1}, but measurements of the peak

(16) The parameters i_p and E_p are respectively the peak current and the peak potential of a redox process: $E_{1/2} = (E_p^a + E_p^c)/2$; E_p^a, i_p^a and E_p^c, i_p^c are respectively the potential and the current of the anodic peak and of the cathodic peak of a reversible process. $\Delta E_p = E_p^a - E_p^c$. An EC process comprises an electron-transfer step (E) followed by a chemical reaction (C). CV stands for cyclic voltammetry, and v (V s^{-1}) is the scan rate in CV experiments.

Scheme 2[a]

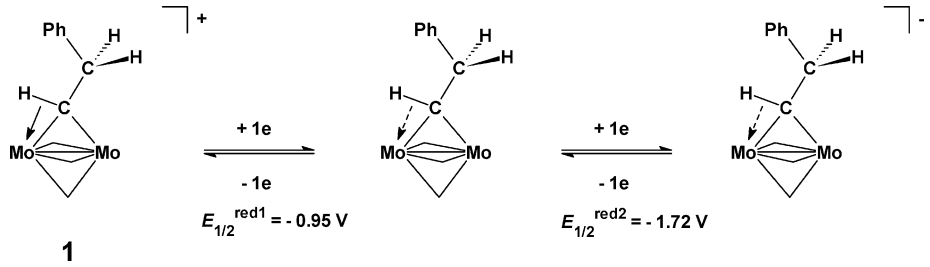

1

[a] Cp rings and SMe bridges are omitted.

Table 4. Crystal Data for Complexes 2 and 3

	2	**3**
formula	$C_{22}H_{28}Mo_2S_3$	$C_{22}H_{30}Mo_2S_3$
M_r	580.50	582.52
cryst size/mm	0.40 × 0.07 × 0.06	0.20 × 0.18 × 0.15
cryst syst	orthorhombic	monoclinic
Space group	$P2_12_12_1$	$P2_1/n$
a/Å	7.9181(2)	9.269(5)
b/Å	13.6483(4)	8.706(2)
c/Å	20.6495(6)	29.196(5)
β/deg		93.622(4)
V/Å^3	2231.6(1)	2351(1)
Z	4	4
D_c/Mg m^{-3}	1.728	1.646
T/K	100	293
μ/mm^{-1}	1.410	1.339
θ(Mo Kα)$_{max}$/deg	24.9	28.4
no. of rflns collected	9106	11 234
no. of unique data/params	2211/209	5005/244
R_{int}	0.047	0.149
no. of obsd rflns ($I > 2\sigma(I)$)	2125	2765
R1 ($I > 2\sigma(I)$)	0.0378	0.070
R1 (all data)	0.0398	0.137
wR2 (all data)	0.0952	0.209
$\Delta\rho_{max}$, $\Delta\rho_{min}$/e Å^{-3}	0.63, −0.93	1.75, −0.89

current ratio $((i_p^a/i_p^c)^{red} < 1$, $(i_p^a/i_p^c)^{red}$ approaches unity with increasing scan rate) indicate that the electron transfers are followed by chemical reactions (EC process)[17] which give products detected by the appearance of oxidation peaks around −0.7 V on the reverse scan. The small reduction observed around −0.5 V (Figure 6) is assigned to the presence of $\mathbf{E}^+$ as an inseparable impurity (about 5−10%) in the sample of **1**.[13]

Controlled-potential reduction of **1** carried out at 273 K at a potential 200 mV negative to the first reduction process was complete after the passage of ca. 1 F mol^{-1} of **1**. Cyclic voltammetry of the catholyte shows the formation of one or more products having oxidation processes at $E_{1/2}^{ox1} = -0.68$ V and $E_{1/2}^{ox2} =$ 0.5 V: i.e., similar to those of the μ-σ,π vinyl (**2**) and μ-alkyl complexes (**3**) (Table 5). It should be noted that the second oxidation of **2** is reversible, while that of **3** is not. The nature of the products formed upon electrochemical reduction of **1** was confirmed by comparison of the ^{1}H NMR spectrum of the solid isolated from the catholyte after removal of the supporting electrolyte with ^{1}H NMR spectra of authentic samples of **2** and **3** with R = Ph. The ^{1}H NMR spectrum showed the presence of both **2** and **3** (60% and 35%, respectively), along with minor amounts (ca. 5%) of the μ-alkylidyne complex $\mathbf{E}$[18] and of $[Mo_2Cp_2(\mu\text{-SMe})_3(\mu\text{-Cl})]$.[2e,19] The latter probably arose from reaction of either **2** or **3** with the dichloromethane solvent.

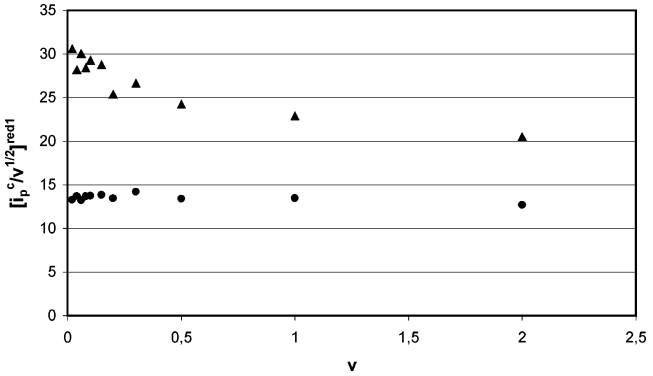

Figure 7. Scan rate dependence of the current function $[i_p^c/v^{1/2}]^{red1}$ for a CH_2Cl_2−$[NBu_4][PF_6]$ solution of $[Mo_2Cp_2(\mu\text{-SMe})_3(\mu\text{-}\eta^1\text{:}\eta^2\text{-CHCH}_2\text{Ph})]^+$ (**1**): (a; ●) in the absence of 2 equiv of HBF_4/Et_2O; (b; ▲) in the presence of 2 equiv of HBF_4/Et_2O.

Since the major products formed during the electrolysis of **1** were shown above to result either from the deprotonation of **1** or from the addition of H$^-$ (or H$^+$ + 2e) to **1**, an ECE mechanism involving a "father−son", acid−base reaction between **1** and its reduced form can be envisaged (Scheme 3). This type of reaction, which may involve a proton-transfer relay,[20] results from an increase in the basicity of the complex as a consequence of one-electron reduction.

The current function $i_p^{red}/v^{1/2}$ is essentially independent of scan rate (Figure 7a) and shows no clear evidence for an ECE process. However, such a process could be obscured by the effect on the magnitude of the reduction current (i_p^{red}) both of the chemical step, which consumes starting material, and of the reduction of $\mathbf{3}^+$, which causes the transfer of a second electron. The mechanism in Scheme 3 was therefore investigated by digital simulations of CV at different scan rates using DigiElch.[21] This showed that the current function was almost independent of v for several sets of values for the equilibrium and rate constants of the "father−son"

(17) (a) Bard, A. J.; Faulkner, L. R. In *Electrochemical Methods: Fundamentals and Applications*; Wiley: New York, 1980; Chapter 11, p 429. (b) Brown, E. R.; Large, R. F. In *Techniques of Chemistry*; Weissberger, A., Ed.; Wiley: New York, 1971; Vol. 1 (Physical Methods of Chemistry), Part II A, Chapter 6, p 423.

(18) The presence of **E** in the catholyte results from the reduction of $\mathbf{E}^+$, present as an inseparable impurity in the samples of **1**.[13]

(19) (a) Gomes de Lima, M. B.; Guerchais, J. E.; Mercier, R.; Pétillon, F. Y. *Organometallics* **1986**, *5*, 1952. (b) Barrière, F.; Le Mest, Y.; Pétillon, F. Y.; Poder-Guillou, S.; Schollhammer, P.; Talarmin, J. *J. Chem. Soc., Dalton Trans.* **1996**, 3967.

(20) Alias, Y.; Ibrahim, S. K.; Queiros, M. A.; Fonseca, A.; Talarmin, J.; Volant, F.; Pickett, C. J. *J. Chem. Soc. Dalton Trans.* **1997**, 4807.

(21) (a) DigiElch can be downloaded from www.DigiElch.de. (b) Rudolph, M. *J. Electroanal. Chem.* **2003**, *543*, 23. (c) Rudolph, M. *J. Electroanal. Chem.* **2004**, *571*, 289. (d) Rudolph, M. *J. Comput. Chem.* **2005**, *26*, 619. (e) Rudolph, M. *J. Comput. Chem.* **2005**, *26*, 633.

Table 5. Redox Potentials of Complexes 1−3 As Measured by Cyclic Voltammetry in CH_2Cl_2−[NBu_4][PF_6][a]

complex	$E_{1/2}^{red1}$/V	$E_{1/2}^{red2}$/V	$E_{1/2}^{ox1}$/V	$E_{1/2}^{ox2}$/V
$[Mo_2Cp_2(\mu\text{-}SMe)_3(\mu\text{-}\eta^1\text{:}\eta^2\text{-}CHCH_2Ph)]^+$ (**1**)	−0.95	−1.72	0.56 (irr)	0.81 (irr)
$[Mo_2Cp_2(\mu\text{-}SMe)_3(\mu\text{-}\eta^1\text{:}\eta^2\text{-}CH{=}CHPh]$ (**2**)			−0.68	0.5
$[Mo_2Cp_2(\mu\text{-}SMe)_3(\mu\text{-}CH_2CH_2Ph)]$ (**3**)			−0.68	0.5 (irr)

[a] Scan rate 0.2 V s^{-1}; potentials are in V vs Fc.

Scheme 3

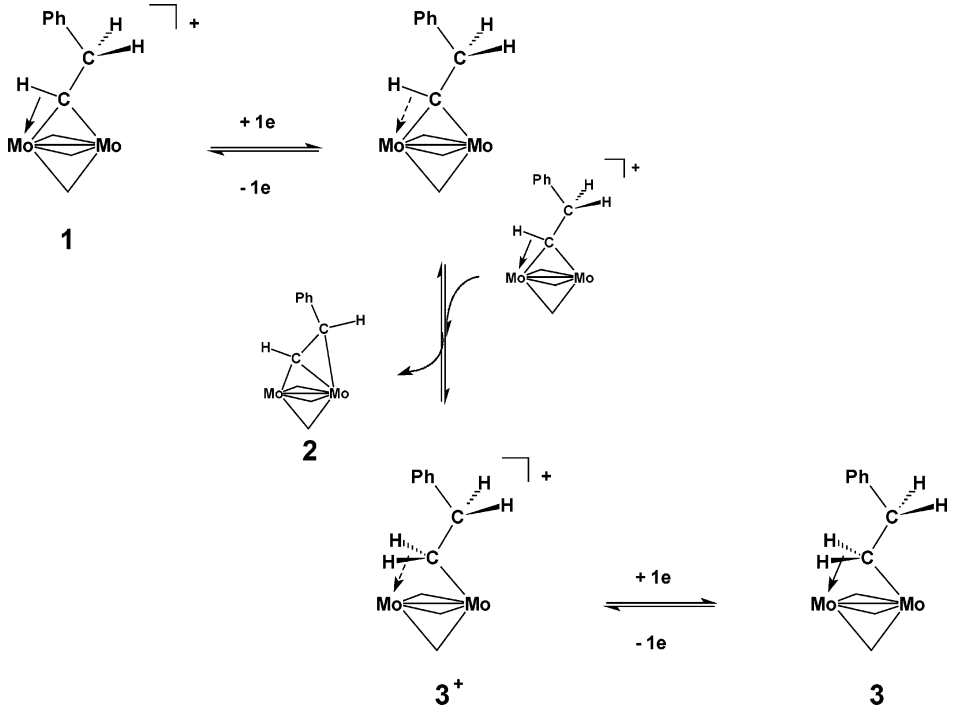

Scheme 4

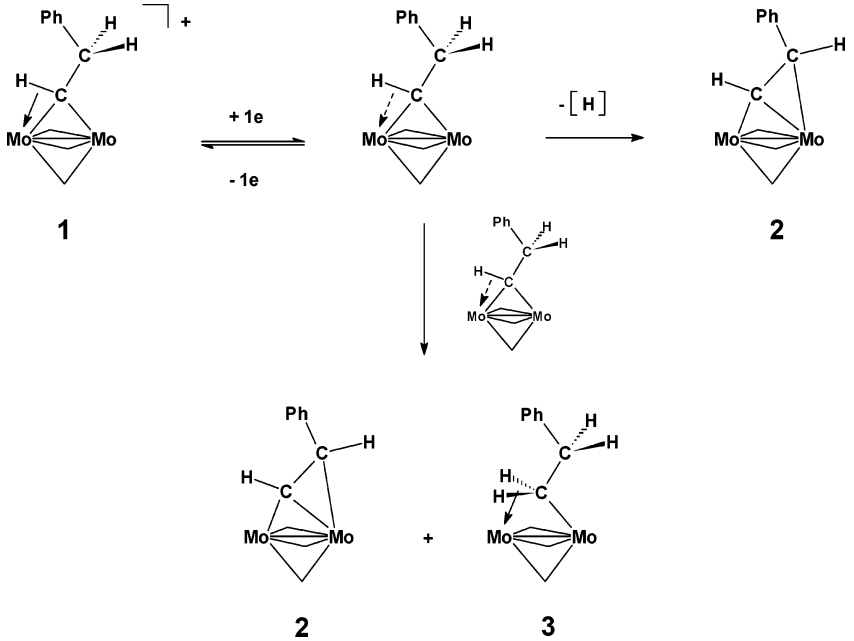

reaction. The occurrence of an ECE-type process therefore cannot be ruled out solely on the basis of the scan-rate dependence of the current function. However, this process would produce equivalent amounts of **2** and **3**, which is not consistent with the experimental results.

An alternative explanation for the formation of **2** and **3** involves H atom transfers. Previously it was reported that the electrochemical reduction of a μ_2-ethylidyne cation gave rise to neutral μ_2-vinylidene and μ_2-ethylidene species via hydrogen atom transfer between two μ_2-ethylidyne radicals.[22] In the present case H atom transfer between two μ-alkylidene radicals would produce equivalent amounts of **2** and **3**, while H atom loss

(22) Aase, T.; Tilset, M.; Parker, V. D. *Organometallics* **1989**, *8*, 1558.

Scheme 5

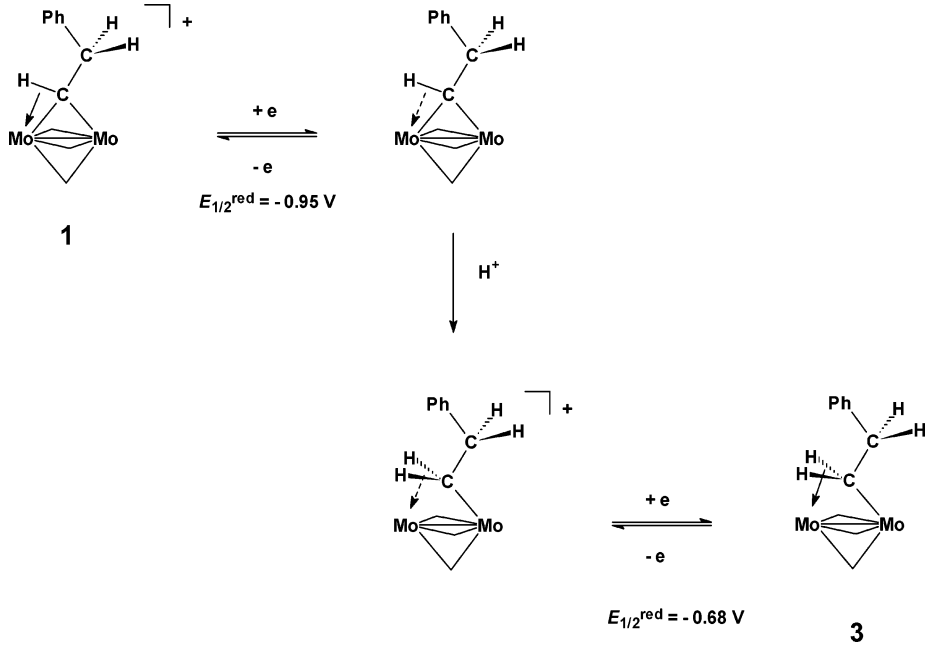

from the reduced form of **1** might contribute to the formation of **2** in more than 50% yield (Scheme 4). This possibility is supported by the results of controlled-potential electrolysis using a solution in which the concentration of **1** had been halved; under these circumstances **2** was shown by ^{1}H NMR to be formed in about 80% yield along with $[Mo_2Cp_2(\mu\text{-}SMe)_3(\mu\text{-}Cl)]$ (ca 20%). **3** could not be detected by ^{1}H NMR of the residue under these conditions.

It is difficult to discriminate between the mechanisms in Schemes 3 and 4 when the electrochemical reduction of **1** is carried out in the absence of acid; it is possible that they may both operate. However, an ECE mechanism is expected when the reaction occurs in the presence of protons. Indeed, upon addition of acid (1 equiv of HBF_4/Et_2O) to a $CH_2Cl_2-[NBu_4][PF_6]$ solution of **1**, CV shows that the current of the first reduction increases while that of the second decreases, consistent with the occurrence of an ECE process (Figure 8b). Furthermore, the variations of the current function $i_p^{red}/v^{1/2}$ against v deviate markedly from linearity at slow scan rates (Figure 7b), again confirming that the reduction of **1** in the presence of acid occurs according to an ECE process (Scheme 5).[17]

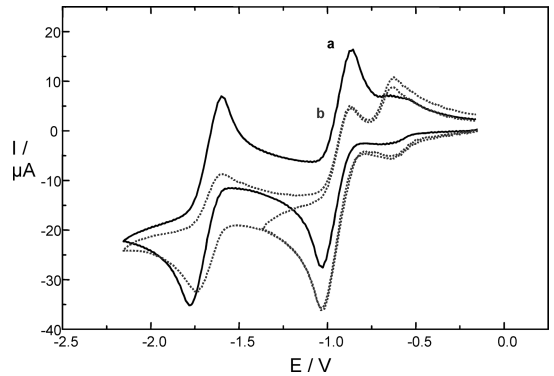

Figure 8. Cyclic voltammetry of $[Mo_2Cp_2(\mu\text{-}SMe)_3(\mu\text{-}\eta^1\text{:}\eta^2\text{-}CHCH_2Ph)]^+$ (**1**; 1 mM) at 0 °C (vitreous carbon electrode, v = 0.2 V s^{-1}): (a) in the absence of acid; (b) after addition of 1 equiv of HBF_4/Et_2O in $CH_2Cl_2-[NBu_4][PF_6]$.

Controlled-potential reduction of **1** in the presence of 1 equiv of HBF_4/Et_2O (1.7 F mol^{-1} of **1**) leads to the formation of **3** as the major product (80%), as shown by the ^{1}H NMR spectrum of the solid residue separated from the supporting electrolyte. The presence of complexes **2**, **E**,[18] and $[Mo_2Cp_2(\mu\text{-}SMe)_3(\mu\text{-}Cl)]$ (ca. 10%, 5%, and 5%, respectively) in the residue was also detected. Electrolyses performed in the presence of 2 equiv of HBF_4/Et_2O produced **3** (ca. 70%) and $[Mo_2Cp_2(\mu\text{-}SMe)_3(\mu\text{-}Cl)]$ (30%) after the transfer of 2.2 F mol^{-1} of **1**. The increase in the amount of the μ-chloro complex is tentatively assigned to reactions of **2** and **3** with protons leading to the release of the hydrocarbyl ligands and binding of a chlorine atom from the solvent. In agreement with this, controlled-potential electrolysis of **1** in the presence of 2 equiv of CF_3CO_2H produces **3** (75%)[23] and the known trifluoroacetato-bridged complex $[Mo_2Cp_2(\mu\text{-}SMe)_3(\mu\text{-}\eta^1\text{:}\eta^1\text{-}OCOCF_3)]$ (25%),[23] characterized by its first oxidation at $E_{1/2}^{ox1} = -0.35$ V,[24] after the passage of ca. 1.9 F mol^{-1} of **1**. The formation of the latter indicates the lability of the hydrocarbyl ligand in species formed as intermediates or product (**2**) of controlled-potential electrolyses of **1**.

Conclusion

We have shown that well-defined transformations of the bridging alkylidene complex $[Mo_2Cp_2(\mu\text{-}SMe)_3(\mu\text{-}\eta^1\text{:}\eta^2\text{-}CHCH_2Tol)](BF_4)$ (**1**) can be carried out by chemical methods to afford the μ-vinyl and μ-alkyl species **2** and **3**. Spectroscopic, X-ray diffraction, and theoretical methods lead to consistent conclusions regarding the structures of the new complexes. In particular, theoretical

(23) The yields of the products formed upon controlled-potential reduction were calculated by comparing the CV peak currents of the products to the reduction peak current of **1** before addition of acid and electrolysis, assuming identical diffusion coefficients.

(24) Le Hénanf, M.; Le Roy, C.; Muir, K. W.; Pétillon, F. Y.; Schollhammer, P.; Talarmin, J. *Eur. J. Inorg. Chem.* **2004**, 1687.

calculations support strongly a η^1 agostic mode of coordination in **1**, for which a diffraction study was unobtainable. For the semibridging alkyl complex [$Mo_2Cp_2(\mu\text{-}SMe)_3(\mu\text{-}CH_2CH_2Tol)$] (**3**) theoretical calculations confirm the heavy-atom skeleton determined by X-ray diffraction and predict a η^1 agostic coordination for the bridging group. They also allow the fluxionality of **3** to be rationalized. Studies of the electrochemical reduction of the μ-alkylidene derivative **1** in the presence or absence of protons reveal its relationships with the μ-vinyl and μ-alkyl complexes. The products of the electrochemical reduction of the μ-alkylidene derivative **1** depend on whether hydrogen ions are freely available: in the presence of acid the μ-alkyl complex **3** is the major product; in the absence of acid the μ-vinyl species **2** is formed in addition to **3** and the product ratio **2**:**3** increases as the starting concentration of **1** is decreased.

Experimental Section

General Procedures and Materials. All reactions were performed under an atmosphere of argon or dinitrogen using conventional Schlenk techniques. Solvents were deoxygenated and dried by standard methods. Literature methods were used for the preparation of [$Mo_2Cp_2(\mu\text{-}SMe)_3(\mu\text{-}CHCH_2R)$]$BF_4$ (**1**).[6a] All other reagents were purchased commercially. Yields of all products are relative to the starting dimolybdenum complexes. Column chromatography was carried out with silica gel purchased from SDS. Chemical analyses were performed either by the Service de Microanalyse ICSN, Gif sur Yvette, France, or by the Centre de Microanalyses du CNRS, Vernaison, France. IR spectra were recorded on a Nicolet-Nexus FT IR spectrometer from KBr pellets. The NMR spectra (^1H, ^{13}C), in $CDCl_3$ or C_6D_6 solutions, were recorded with a Bruker AC 300 or AMX 400 spectrometer and were referenced to $SiMe_4$. $^1H-^{13}C$ 2D experiments were carried out on a Bruker DRX 500 spectrometer. The preparation and the purification of the supporting electrolyte [NBu_4][PF_6] and the electrochemical equipment were as described previously.[25] All of the potentials (text, tables, figures) are quoted against the ferrocene−ferrocenium couple; ferrocene was added as an internal standard at the end of the experiments.

Reaction of 1 with Butyllithium. Complex **1** (0.1 g, 1.5 mmol) and 1.5 equiv of *n*-butyllithium (V = 900 μL, 2.5 M solution in hexane) were stirred in tetrahydrofuran (30 mL) at 0 °C for 20 min. The solution turned color from brown to purple. After evaporation of the solvents, **2** was extracted with diethyl ether (3 × 10 mL). Evaporation of the volatiles and washing of the residue with cold pentane afforded **2** as a purple solid (0.08 g, 92% yield).

2. ^1H NMR (C_6D_6, 25 °C; δ): 7.18 (d, 1H, J_{HH} = 15.0 Hz, Tol-CH=C*H*−Mo), 7.04 (d, 2H, J_{HH} = 7.8 Hz, $CH_3C_6H_4$), 6.92 (d, 2H, J_{HH} = 7.8 Hz, $CH_3C_6H_4$), 6.73 (d, 1H, J_{HH} = 15.0 Hz, Tol-C*H*=CH−Mo), 4.97 (s, 10H, C_5H_5), 2.06 (s, 3H, $CH_3C_6H_4$) 1.70 (s, 3H, SC*H*$_3$), 1.58 (s, 3H, SC*H*$_3$), 1.54 (s, 3H, SC*H*$_3$). $^{13}C\{^1H\}$ NMR (C_6D_6, 25 °C; δ): 153.8 (Tol-CH=*C*H−Mo), 139.1, 136.6, 129.4, 127.5 ($CH_3C_6H_4$), 104.8 (Tol-*C*H=CH−Mo), 91.0 (C_5H_5), 21.1 ($CH_3C_6H_4$), 16.3 (S*C*H$_3$), 10.2 (S*C*H$_3$), 9.8 (S*C*H$_3$). Anal. Calcd for $C_{22}H_{28}Mo_2S_3$: C, 45.5; H, 4.9. Found: C, 45.5; H, 4.9.

2 (R = Ph). ^1H NMR (C_6D_6, 25 °C; δ): 7.21 (d, 1H, J_{HH} = 15.0 Hz, Ph-CH=C*H*−Mo), 7.16−7.06 (m, 5H, C_6H_5), 6.68 (d, 1H, J_{HH} = 15.0 Hz, Ph-C*H*=CH−Mo), 4.97 (s, 10H, C_5H_5), 1.72 (s, 3H, SC*H*$_3$), 1.54 (s, 3H, SC*H*$_3$), 1.49 (s, 3H, SC*H*$_3$).

Reaction of 1 with $NaBH_4$. A solution of complex **1** (0.1 g, 0.15 mmol) in tetrahydrofuran (30 mL) was stirred in the presence of 3 equiv of $NaBH_4$ (0.017 g) for 1 h at room temperature. The solution readily turned color from brown to green. The solvent was then removed under vacuum, and the organometallic products were extracted with diethyl ether (2 × 20 mL). After evaporation of the diethyl ether, the residue was chromatographed on a silica gel column. Elution with a mixture of CH_2Cl_2/hexane (1:4) afforded a green solution of **3**, which was evaporated under vacuum. Compound **3** was obtained as a green powder (0.025 g, 29% yield).

3. ^1H NMR (toluene-d_8, 25 °C; δ): 6.96 (d, 2H, J_{HH} = 7.8 Hz, $CH_3C_6H_4$), 6.85 (d, 2H, J_{HH} = 7.8 Hz, $CH_3C_6H_4$), 5.05 (s, 10H, C_5H_5), 2.42 (*p*t, 2H, J_{HH} = 6.6 Hz, Tol-C*H*$_2$CH$_2$−Mo) 2.15 (s, 3H, C*H*$_3$C$_6$H$_4$), 1.71 (s, 3H, SC*H*$_3$), 1.64 (s, 3H, SC*H*$_3$), 1.17 (s, 3H, SC*H*$_3$), −5.57 (br, 2H, Tol-CH$_2$C*H*$_2$−Mo). $^{13}C\{^1H\}$ NMR (toluene-d_8, 25 °C; δ): [139−125] ($CH_3C_6H_4$), 90.0 (C_5H_5), 34.4 (Tol-*C*H$_2$CH$_2$−Mo), 21.1 (*C*H$_3$C$_6$H$_4$), 12.3 (S*C*H$_3$), 11.8 (S*C*H$_3$), 10.9 (S*C*H$_3$), 1.9 (Tol-CH$_2$*C*H$_2$−Mo). Anal. Calcd for $C_{22}H_{30}Mo_2S_3$, 1/4 CH_2Cl_2: C, 44.2; H, 5.1. Found C, 44.0; H, 5.2.

3 (R = Ph).^1H NMR (tol-d_8, 25 °C; δ): 7.12−6.90 (m, 5H, −C_6H_5), 5.04 (s, 10H, C_5H_5), 2.42 (*p*t, 2H, Ph-C*H*$_2$CH$_2$−Mo), 1.71 (s, 3H, SC*H*$_3$), 1.65 (s, 3H, SC*H*$_3$), 1.15 (s, 3H, SC*H*$_3$), −5.58 (br, 2H, Ph-CH$_2$C*H*$_2$−Mo).

Controlled-Potential Electrolyses of 1. (a) In the Absence of Acid. A 16.5 mg portion (2.5 × 10^{-5} mol) of complex **1** was dissolved in 15 mL of CH_2Cl_2−[NBu_4][PF_6] under N_2, and the potential of the Pt cathode was set at −1.2 V. The electrolysis was completed after transfer of 2.2 C (0.9 F mol^{-1} of **1**). The catholyte was cannulated in a Schlenk flask and the solvent removed under reduced pressure. A 10 mL portion of pentane was then added to the solid residue, and the mixture was stirred for 10 min before being filtered. The filtrate was dried under vacuum. The solid residue was dissolved in C_6D_6, and the products formed by electrolysis were characterized by ^1H NMR.

(b) In the Presence of HBF_4/Et_2O. In a typical experiment, to 13.9 mg (2.1 × 10^{-5} mol) of **1** dissolved in 15 mL of CH_2Cl_2−[NBu_4][PF_6] under N_2 was added 2 equiv of HBF_4/Et_2O. The controlled-potential electrolysis was performed at −1.2 V. The catholyte was treated as above.

Crystal Structure Determinations of 2 and 3. Pertinent data are summarized in Table 4. Measurements for **2** were made at 100 K on a Nonius KappaCCD diffractometer, while those for **3** were made at room temperature on a Nonius CAD4 diffractometer. Mo Kα radiation (λ = 0.710 73 Å) was used in both experiments. The structures were solved and refined by standard procedures.[26] H atoms were positioned using stereochemical considerations, the orientations of methyl groups being initially obtained from difference maps, and then rode on their parent carbon atoms.

Molecules of **2** are disordered over two sites related approximately by the pseudosymmetrical mirror operation 1.5 − x, y, z. The main structure with occupancy 0.764(3) is shown in Figure 2. Cp and phenyl rings were refined as regular polygons, and anisotropic vibration tensors were refined only for Mo and S atoms. This model, the best of several that were considered, was refined satisfactorily with data averaged assuming *mmm* Laue symmetry (see Table 4). Although the overlapping of the molecular images obscures the finer details of the structure, in particular the position of the H atom attached to C(4), we consider that the main features of the heavy-atom skeleton are reliably established. The disorder seems to be a general feature of the crystals, since data sets from three different specimens gave essentially the same results. For **3** the crystals were small and of poor quality. Refinement using a conventional model (U^{ij} tensors for all non-H atoms) established the heavy-atom skeleton but did not yield experimental positions for the C(4) H atoms.

(25) Cabon, J. Y.; Le Roy, C.; Muir, K. W.; Pétillon, F. Y.; Quentel, F.; Schollhammer, P.; Talarmin, J. *Chem. Eur. J.* **2000**, *6*, 3033.

(26) Programs used: (a) Sheldrick, G. M. SHELX97; University of Göttingen, Göttingen, Germany, 1998. (b) Farrugia, L. J. WinGX-A Windows Program for Crystal Structure Analysis. *J. Appl. Crystallogr.* **1999**, *32*, 837.

Computational Methods. All calculations were carried out using the Gaussian 03 program, Revision A.7.[27] The B.03LYP functional was used throughout,[28] and the molybdenum and sulfur atoms were represented by the LANL2 effective core potential and its associated basis set,[29] augmented by f and d polarization functions, respectively.[30] The 6-31G* basis set was used for all other atoms, with the exception of the hydrogens on the α-carbon (those potentially involved in agostic interactions), which were described with a 6-311G** basis. Full optimizations were performed without constraint, and vibrational frequencies were calculated to confirm the nature of the stationary points in each case.

Acknowledgment. We are grateful to N. Kervarec and Dr. R. Pichon for recording two-dimensional NMR spectra on a Bruker DRX 500 (500 MHz) spectrometer. We thank the CNRS, the EPSRC, and the Universities of Glasgow, York, and Brest for financial support.

Supporting Information Available: Tables giving structures and total energies of all stationary points reported and CIF files giving crystallographic data for **2** and **3**. This material is available free of charge via the Internet at http://pubs.acs.org. Crystallographic data for **2** and **3** have also been deposited with the Cambridge Crystallographic Data Centre as CCDC 279840 and 279841. Copies can be obtained free of charge on application to the CCDC, 12 Union Road, Cambridge CB2 1EZ, U.K. (fax, international + 44(0) 1223/336-033; e-mail, deposit@ccdc.com.ac.uk).

OM050761G

(27) Frisch, M. J.; Trucks, G. W.; Schlegel, H. B.; Scuseria, G. E.; Robb, M. A.; Cheeseman, J. R.; Montgomery, J. A., Jr.; Vreven, T.; Kudin, K. N.; Burant, J. C.; Millam, J. M.; Iyengar, S. S.; Tomasi, J.; Barone, V.; Mennucci, B.; Cossi, M.; Scalmani, G.; Rega, N.; Petersson, G. A.; Nakatsuji, H.; Hada, M.; Ehara, M.; Toyota, K.; Fukuda, R.; Hasegawa, J.; Ishida, M.; Nakajima, T.; Honda, Y.; Kitao, O.; Nakai, H.; Klene, M.; Li, X.; Knox, J. E.; Hratchian, H. P.; Cross, J. B.; Bakken, V.; Adamo, C.; Jaramillo, J.; Gomperts, R.; Stratmann, R. E.; Yazyev, O.; Austin, A. J.; Cammi, R.; Pomelli, C.; Ochterski, J. W.; Ayala, P. Y.; Morokuma, K.; Voth, G. A.; Salvador, P.; Dannenberg, J. J.; Zakrzewski, V. G.; Dapprich, S.; Daniels, A. D.; Strain, M. C.; Farkas, O.; Malick, D. K.; Rabuck, A. D.; Raghavachari, K.; Foresman, J. B.; Ortiz, J. V.; Cui, Q.; Baboul, A. G.; Clifford, S.; Cioslowski, J.; Stefanov, B. B.; Liu, G.; Liashenko, A.; Piskorz, P.; Komaromi, I.; Martin, R. L.; Fox, D. J.; Keith, T.; Al-Laham, M. A.; Peng, C. Y.; Nanayakkara, A.; Challacombe, M.; Gill, P. M. W.; Johnson, B.; Chen, W.; Wong, M. W.; Gonzalez, C.; Pople, J. A. *Gaussian 03*, revision B.03; Gaussian, Inc.: Wallingford, CT, 2004.

(28) (a) Becke, A. D. *Phys. Rev. A* **1988**, *38*, 3098. (b) Lee, C.; Yang, W.; Parr, R. G. *Phys. Rev. B* **1988**, *37*, 785. (c) Becke, A. D. *J. Chem. Phys.* **1993**, *98*, 5648.

(29) Wadt, W. R.; Hay, P. J. *J. Chem. Phys.* **1985**, *82*, 284.

(30) (a) Ehler, A. W.; Bohme, M.; Dapprich, S.; Gobbi, A.; Hollwarth, A.; Jonas, V.; Kohler, K. F.; Stegmann, R.; Velkamp, A.; Frenking, G. *Chem. Phys. Lett.* **1993**, *208*, 111. (b) Hollwarth, A.; Bohme, M.; Dapprich, S.; Ehlers, A. W.; Gobbi, A.; Jonas, V.; Kohler, K. F.; Stegmann, R.; Veldkamp, A.; Frenking, G. *Chem. Phys. Lett.* **1993**, *208*, 237.